Synchrotron radiation studies of the orientation of thin silicon phthalocyanine dichloride film on HOPG substrate*

DENG Ju-Zhi(邓居智)[1,2;1)] CHEN Rong(陈荣)[1] SEKIGUCHI Tetsuhiro[3]
BABA Yuji[3] HIRAO Norie[3] HONDA Mitsunori[3]

1 (Key Laboratory of Nuclear Resources and Environment (East China Institute of Technology), Ministry of Education, Nanchang 330013, China)
2 (School of Geophysics and Information Technology, China University of Geosciences(Beijing), Beijing 100083, China)
3 (Synchrotron Radiation Research Center, Japan Atomic Energy Agency, Ibaraki-ken 319-1195, Japan)

Abstract Thin silicon phthalocyanine dichloride films on HOPG were prepared and the sample was heated in the vacuum with laser. The thickness of the thin sample on HOPG was checked by X-ray photoemission spectroscopy. The orientation of the molecules in respect to the substrate plane was investigated by measuring the silicon K-edge near edge X-ray absorption fine structure (NEXAFS). In the NEXAFS spectra of the thin sample, two clear peaks which were assigned to $1s \rightarrow \sigma^*_{\text{Si-N}}$ and $1s \rightarrow \sigma^*_{\text{Si-Cl}}$ appeared around 1847.2 eV and 1843.1 eV respectively. The intensities of the resonance peaks showed strong polarization dependence. A quantitative analysis of the polarization dependence revealed that the Si–N bond tended to lie down while the Si–Cl bond was out of the molecular plane.

Key words near edge X-ray absorption fine structure (NEXAFS), orientation, silicon phthalocyanine dichloride, polarization dependence

PACS 31.15.aP, 32.30.Rj, 34.35.+a

1 Introduction

In recent years, organic semiconducting thin films have become increasingly important for the possible application of these films in several fields such as electronics, opto-electronics and gas sensing[1, 2]. The family of the phthlocyanines (Pcs) represents one of the most promising candidates for ordered organic thin films in organic electronics, as these systems possess advantageous attributes such as chemical stability, excellent film growth and electronic properties[3, 4]. It has been already concluded that the ordering and orientation of the Pcs represents one of the most promising candidates for organic thin films[5]. Anisotropic electrical transport properties are often observed in these materials; they are caused by the preferred orientation of the molecules[6—8]. Especially for Pcs, a very high degree of orientation in evaporated films was observed on several substrates[9, 10]. But very few studies have attempted to clarify the ordering and orientation of silicon phthalocyanine dichloride ($SiPcCl_2$).

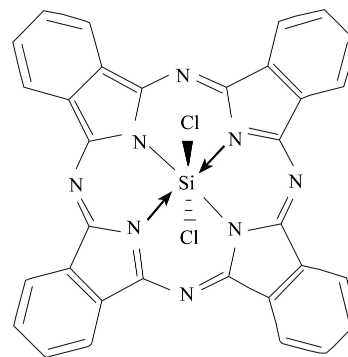

Fig. 1. Molecular structure of $SiPcCl_2$.

In the present work, therefore, we investigated the electronic structure and orientation nature of

Received 15 October 2007, Revised 3 January 2008
* Supported by Nuclear Researchers Exchange Program 2005 and Photon Factory Program Advisory Committee (2004G340)
1) E-mail: jzdeng73@yahoo.com.cn

$SiPcCl_2$ molecular films on highly oriented pyrolitic graphite (HOPG) substrate using polarization dependent near-edge X-ray absorption fine-structure (NEXAFS).

In the molecular structure of $SiPcCl_2$ (Fig. 1), a Si atom is located in the center of the planar phthalocyanine (Pc) ring, with two Cl atoms attached to the Si atom above and below the SiPc plane.

2 Experiments

The experiments were performed at the end station of the beam line BL27A of the photon factory in the High Energy Accelerator Research Organization (KEK-PF), Tsukuba, Japan. The beam line was equipped with an InSb(111) double crystal monochromator. The energy resolution from the monochromator was 0.85 eV at 1.84 keV (Si K-edge). The synchrotron beam was generated in the bending magnet, and it was linearly polarized in the horizontal direction. The end station has two vacuum chambers: (1) the main chamber and (2) the preparation chamber: the base pressure of both chambers is in the order of 10^{-8} Pa. The main chamber consists of a hemispherical electron energy analyzer (VSW Co. Class-100) for XPS measurements, a manipulator and a laser annealing system. The preparation chamber is equipped with thin film evaporators, thickness monitor and transfer system[11].

Powder samples of $SiPcCl_2$ and 12 mm×12 mm HOPG were purchased from Sigma-Aldrich Co. and Tomoe Co. respectively. The HOPG substrates were cleaned with acetone by ultrasonication before use. A 100 mM $SiPcCl_2$ solution was made by dissolving $SiPcCl_2$ powder in hexane. A little amount of the solution was dropped homogeneously on the HOPG surface. In addition, the sample was heated at 345 ℃ for 5 minutes in the vacuum with laser after the solution was dried naturally in the vacuum.

The NEXAFS spectra were taken by the total electron yields, which were monitored by sample drain current. Si K-edge NEXAFS spectra were measured for the thin $SiPcCl_2$ film on HOPG after heating in the vacuum. In order to compare the spectral features, the NEXAFS spectra of $SiPcCl_2$ without heating were also taken for the reference.

3 Results and discussion

3.1 X-ray photoelectron spectra

Figure 2 shows the XPS wide scan excited by 3200 eV photons for the sample. First, we will estimate the thickness d of the sample[12]. The intensity of the Si 1s photoelectron I (Si 1s) is expressed as

$$I(\mathrm{Si1}s) = K\sigma(\mathrm{Si1}s)\lambda_{\mathrm{SiPcCl_2}}(\mathrm{Si1}s)n_{\mathrm{SiPcCl_2}}(\mathrm{Si})\times \left[1-\exp\left\{\frac{-d}{\lambda_{\mathrm{SiPcCl_2}}(\mathrm{Si1}s)}\right\}\right] \quad (1)$$

where K is constant depending in the detection efficiency and X-ray flux, $\sigma(\mathrm{Si1}s)$ is photo ionization cross section of Si 1s at 3200 eV photons, $\lambda_{\mathrm{SiPcCl_2}}(\mathrm{Si1}s)$ is inelastic mean free path (IMFP) of Si 1s photoelectron in $SiPcCl_2$ and n(Si) is the atomic concentration of silicon in the $SiPcCl_2$ sample. For carbon, the C 1s photoelectrons are emitted from both the substrate and $SiPcCl_2$ sample, so the intensity of the C 1s photoelectron I(C 1s) is calculated as

$$I(\mathrm{C1}s) = K\sigma(\mathrm{C1}s)\lambda_{\mathrm{C}}(\mathrm{C1}s)n_{\mathrm{C}}(\mathrm{Si})\times \exp\left\{\frac{-d}{\lambda_{\mathrm{SiPcCl_2}}(\mathrm{C1}s)}\right\}+ K\sigma(\mathrm{C1}s)\lambda_{\mathrm{SiPcCl_2}}(\mathrm{C1}s)n_{\mathrm{SiPcCl_2}}(\mathrm{C})\times \left[1-\exp\left\{\frac{-d}{\lambda_{\mathrm{SiPcCl_2}}(\mathrm{C1}s)}\right\}\right] \quad (2)$$

where all the parameters are the same as those in Eq. (1). For σ, the reported values were used[13]. Using the TTP-2M equation[14], the values $\lambda_{\mathrm{SiPcCl_2}}$ (Si1s) and $\lambda_{\mathrm{SiPcCl_2}}$ (C1s) were estimated to be 36.556 and 68.18Å respectively. The I(Si)/I(C) ratio as a function of d is shown in the upper side of Fig. 2. The calculated thickness of this sample is 4.287 nm (about five layers molecule).

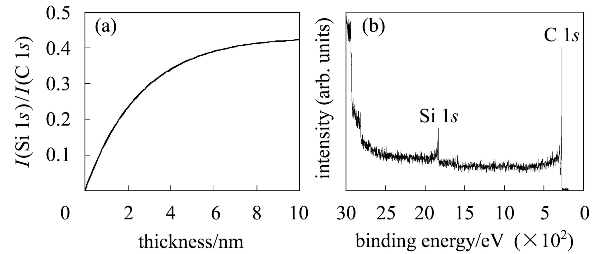

Fig. 2. XPS wide scans exited by 3200eV photons for silicon phthalocyanine dichloride thin sample on HOPG. The relation between film thickness and peak intensity calculated by Eqs. (1) and (2) are shown in the upper side. The thickness of the thin sample obtained from this curve is 4.287 nm.

3.2 Si K-shell NEXAFS spectra

Figure 3 shows the polarization-angle dependence of the Silicon K-edge NEXAFS spectra for the powdered $SiPcCl_2$ sample without heating (marked A) and the thin $SiPcCl_2$ film on HOPG after heating in the vacuum (marked B). The spectra are normalized to the edge jump at the continuum region around 1860 eV where they should show no polarization dependence[15].

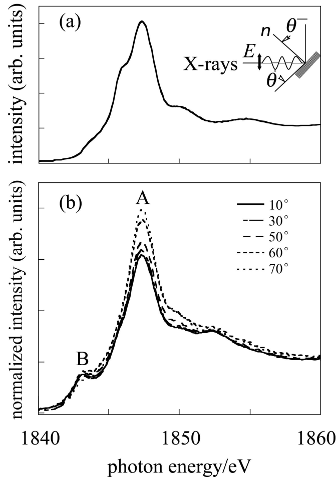

Fig. 3. NEXAFS spectra at the silicon K-edge taken by the total electron yield. (a) thin $SiPcCl_2$ film before heating. (b) polarization dependence for thin $SiPcCl_2$ on HOPG after heating in the vacuum. $\boldsymbol{E}$ is the electric field vector of synchrotron beam and θ is the incident angle defined by the angle between sample surface and synchrotron beam.

For the spectra of the sample without heating, there is no polarization dependence. That is, all of the spectra are the same in different incident angles. While it is noteworthy for the heated sample that a new clear peak is observed at 1843.1 eV (peak B) in addition to a strong feature at 1847.2 eV (peak A), and also that the spectra noticeably depend on the polarization angles. We inferred that the bonding between the substrate and molecules becomes tightened due to the annealing process in the vacuum and this process makes the molecules became oriented.

In order to assign those peaks to correlative chemical bonds, we calculated the unoccupied molecular orbital in the core excited states (Equivalent core approximation)[16] for $SiPcCl_2$ molecule using the self-consistent field molecular orbital (SCF-MO) method with 3-21G basis set. Most stable molecular structures were obtained by optimizing the total potential energy. Based on the calculations, we assign peak A and peak B to in-plane and out-of-plane transitions respectively.

The evidence agrees with the fact that peak A and peak B in Fig. 3(b) can be assigned to Si $1s \rightarrow \sigma^*_{\text{Si-N}}$ (in-plane) and $1s \rightarrow \sigma^*_{\text{Si-Cl}}$ (out-of-plane) transitions, respectively[17].

To determine the average polar angle of Si—Cl bond and the average tilt angle of Si—N bond, the integrated intensities of the $\sigma^*_{\text{Si-Cl}}$ resonance and $\sigma^*_{\text{Si-N}}$ resonance were obtained quantitatively by curve-fitting technique. Using a nonlinear least-square routine, the NEXAFS curves were fitted with a linear combination consisting of four symmetrically broadened Gaussian functions for the resonant features and of a Gaussian-broadened step function for the edge jump[18]. Typical spectral deconvolution is shown in Fig. 4.

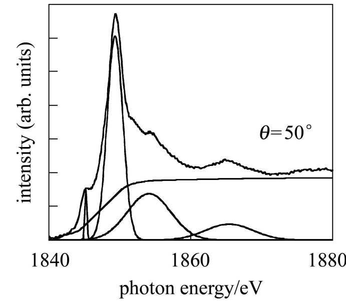

Fig. 4. Spectral deconvolution for the $SiPcCl_2$ on HOPG. The incident angle (θ) was written on the right side of the spectrum. The NEXAFS curves were fitted with linear combination of four symmetrically broadened Gaussian functions for resonant features and a Gaussian-broadened step function for the edge jump.

The remarkable feature observed in peak A and B is the clear polarization dependence of their intensity. The intensity of the peak A increases with the increase in the incident angles of the synchrotron beam. While the intensity of the peak B decreases with the increase in the incident angles of the synchrotron beam. The peak intensity I of the NEXAFS spectra using the synchrotron beam of electric field $\boldsymbol{E}$ is expressed as follows[15]:

$$I \propto |\boldsymbol{E}\cdot\boldsymbol{O}|^2 \propto \cos^2\delta \tag{3}$$

where $\boldsymbol{O}$ is the direction of the final state orbital and δ is the angle between $\boldsymbol{E}$ and $\boldsymbol{O}$. Considering the polarization dependences in Fig. 2, we can suppose that the final state orbital represented by the peak A is parallel to the basal plane of graphite sheet, while that represented by the peak B is perpendicular to the basal plane of graphite. In order to certify those speculations more quantitatively, we will next estimate the angle of Si—N and Si—Cl σ bonds.

For the HOPG substrate, the multilayer films are most unlikely to tend azimuth symmetry, the angle-dependent intensities for $\sigma^*_{\text{Si-N}}$ and $\sigma^*_{\text{Si-Cl}}$ can be expressed by Eqs. (4) and (5) respectively[15].

$$I(\theta,\gamma) = A[P\sin^2\theta\cos^2\gamma - \frac{1}{2}\sin^2\theta\sin^2\gamma + \frac{1}{2}(1-P)(1+\cos^2\gamma)], \tag{4}$$

$$I(\theta,\alpha) = A[P\cos^2\theta\cos^2\alpha + \frac{1}{2}\sin^2\theta\sin^2\alpha + \frac{1}{2}(1-P)(1+\sin^2\alpha)], \tag{5}$$

where A is the normalization factor and $P(=0.9)$[13] is the degree of linear polarization of X-rays and the

tilt angle represents the polar angle of $\sigma^*_{\text{Si-Cl}}$ orbital, namely the angle between the surface normal ($\boldsymbol{n}$) and the $\sigma^*_{\text{Si-Cl}}$ orbital. γ is the tilt angle of molecular plane which contains $\sigma^*_{\text{Si-N}}$ orbital.

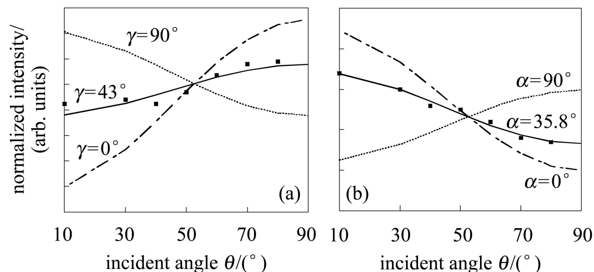

Fig. 5. Plots of intensities, $I(\theta)$ as a function of X-ray incidence (polarization) angle θ. Also shown are the best-fit curves (solid lines) and the hypothetical curves calculated for the angle 0° (chain lines) and 90° (dotted lines) with respect to the surface normal.

Figure 5 shows the $\sigma^*_{\text{Si-N}}$ and $\sigma^*_{\text{Si-Cl}}$ resonance intensities as a function of the polarization angles, θ. The results of curve-fit analysis using plane-type (Eq. (2)) and vector-type equations (Eq. (3)) are also shown. The plane type equation is used for analyzing the in-plane orbital, i.e., $\sigma^*_{\text{Si-N}}$ in our case. The vector equation is adopted for the out-of-plane orbital, i.e., $\sigma^*_{\text{Si-Cl}}$[19]. The average tilted angles of the molecular plane ($\sigma^*_{\text{Si-N}}$) and the Si—Cl bond axis were found to be roughly 43° and 36° to the surface respectively. The average tilted angles deviate from the magic angle (54.7°), which means compared with the randomly oriented molecules, the Si—N bonds tend to lie down on the surface on average. The consistency also corroborates the validity of our resonance assignments.

4 Conclusions

We have prepared thin films sample of SiPcCl_2 by dropping the molecular solution on HOPG and heating the sample in the vacuum at ~345 ℃. We have investigated the orientation and electronic structure of those films on HOPG using polarization dependent NEXAFS. In the Si K-edge NEXAFS spectra for thin film sample, two clear peaks that were assigned to $1s \rightarrow \sigma^*_{\text{Si-N}}$ and $1s \rightarrow \sigma^*_{\text{Si-Cl}}$ appeared around 1847.2 eV and 1843.1 eV. The intensities of the resonance peaks showed strong polarization dependence. The quantities analysis of the polarization dependence revealed that on average the Si—N bond tend to lie down on the surface compared with the randomly oriented molecules, while the Si—Cl bond tends to perpendicular to the molecular plane.

The authors would like to express their gratitude to the staff of the Photon Factory (KEK-PF) for their assistance throughout the experiments.

References

1 Friend R H, Gymer R W, Holmes A B et al. Nature(London), 1999, **121**: 397
2 Dimitrakopoulos C, Malenfant P R L. Adv. Mater (Weinheim, Ger.), 2002, **99**: 14
3 Forrest S R. Chem. Rev., 1996, **97**: 1793
4 Biswas I, Peisert H, Schwieger T et al. J. Chem. Phys., 2005, **122**: 064710
5 Miao P, Robinson A W, Palmer R E. J. Phys. D, 1998, **31**: L37
6 Michaelis W, Wöhrle D, Schlettwein D. J. Mater. Res., 2004, **19**: 2040
7 Ostrick J R, Dodabalapur A, Torsi L et al. J. Appl. Phys., 1997, **81**: 6804
8 Peisert H, Schwiegerm T J, Auerhammerm et al. J. Appl. Phys., 2001, **90**: 466
9 Vearey-Poberts A R, Steiner H J, Evans S et al. Appl. Surf. Sci., 2004, **234**: 131
10 Evans D A, Steiner H J, Vearey-Roberts A R et al. Nucl. Instrum. Methods Phys. Res. B, 2003, **199**: 475
11 Sekiguchi T, Baba Y, Shimoyama I et al. J. Phys.: Condens. Matter, 2005, **17**: 5453
12 Moulder J F, Stichle W F, Sobol P E, Bomben K D. Handbook of X-ray Photoelectron Spectroscopy. Physical Electronics Inc., Eden Prairie, USA, 1995
13 Scofield J H. Physics, 1973, **45**: UC-34
14 Tanuma S, Powell C J, Penn D R. Surf. Interface Anal., 1994, **21**: 165
15 Stöhr J. in: NEXAFS Spectroscopy. Ed. by G. Ertl, R. Gomer, D.L. Mills, H.K.V. Lotsch. Berlin: Springer-Verlag Press, 1992. 71, 276
16 Boo B H, LIU Z Y, Koyano I. J. Phys. Chem. A, 2000, **104**: 1474
17 DENG J Z, Baba Y, Sekiguchi T, Hirao N, Honda M J. Phys.:Condens. Matter, 2007, **19**: 11
18 Outka D A, Stöhr J. J. Chem. Phys., 1988, **88**: 3539
19 Kitamura H. Synchrotron Radiation Calculation Program for PC98, Version 2.3. 1993